

Crystallization and Preliminary Crystallographic Analysis of Thioredoxin-dependent Thiol Peroxidase (SF2523) From *Shigella flexneri* 2a str. 301*

LIU Yong¹⁾, LU Fang²⁾, GUO Gang-Xing¹⁾, FENG Duo¹⁾, ZHANG Bei¹⁾, GAO Wei^{1)**}, BI Ru-Chang³⁾

¹⁾ School of Science, Beijing Forestry University, Beijing 100083, China;

²⁾ College of Forestry, Beijing Forestry University, Beijing 100083, China;

³⁾ Institute of Biophysics, Chinese Academy of Sciences, Beijing 100101, China)

Abstract *Shigella flexneri* was the most common pathogen causing bacillary dysentery. Thioredoxin-dependent thiol peroxidase (SF2523) proteins was from *Shigella flexneri* 2a str. 301. It belonged to thioredoxin peroxidase family and played an important role in protecting the biological macromolecule by scavenging active oxygen generated in the process of aerobic metabolism. To understand the underlying mechanism, prokaryotically expressed thioredoxin-dependent thiol peroxidase protein was purified using affinity chromatography and gel filtration, crystallized using the vapour-diffusion method. The crystal grew in a condition consisting of 1.8 mol/L tri-Ammonium citrate, pH 7.0 using 1 g/L protein solution at 289 K. A complete data set was collected from a crystal to 2.75 Å resolution using synchrotron radiation at 100 K. The crystal belonged to space group P2₁2₁2₁, with unit-cell parameters $a = 35.80$ Å, $b = 50.63$ Å, $c = 88.52$ Å, $\alpha = \beta = \gamma = 90.00^\circ$. One molecule was found in the asymmetric unit with a Matthews coefficient of 2.03 Å³/u, corresponding to a solvent content of 39.56%.

Key words thioredoxin peroxidase, active oxygen, crystal

DOI: 10.16476/j.pibb.2017.0067

Reactive oxygen species (ROS) were produced in aerobic metabolic processes, such as respiration and photosynthesis in mitochondria, chloroplasts and peroxisomes [1]. ROS could cause oxidation of membrane phospholipids, because the polyunsaturated fatty acids in biological membrane phospholipids contained many double bonds [2]. It also caused DNA mutations by inducing the cleavage or cross-linking of single or double strand [3]. Carbonyl derivative was generated when ROS attacked the protein, which could change the protein tertiary structure, lead to the extension of protein and form potentially harmful crosslinked product [4].

In order to reduce the amount of ROS, aerobic organisms were equipped with an array of antioxidant systems [5]. Peroxiredoxin (Prx) was an important antioxidant that widely existed in eubacteria, archaea, yeast, algae, higher plants and mammals [6-7]. Different

from other oxide enzyme, Prx used active cysteine residues in the biochemical reaction, rather than redox cofactors like agon or metal ion [8]. According to the number and location of catalytic cysteines, Prx proteins could be divided into three categories: typical 2-cys, atypical 2-cys and 1-cys [9].

The research object of this article was thioredoxin-dependent thiol peroxidase (SF2523) from *Shigella flexneri* 2a str. 301, it consisted of 156 amino acids, in which 4 to 156 amino acid residues formed

*This work was supported by grants from The Fundamental Research Funds for the Central Universities (2015ZCQ-LY-02) and The National Natural Science Foundation of China (31070651).

**Corresponding author.

Tel: 86-10-62338136, E-mail: w_gao@bjfu.edu.cn

Received: September 8, 2016 Accepted: March 6, 2017

thioredoxin domain. The 45th and 50th cysteine residues formed intramolecular disulfide bonds. Redox reaction ($2R'-SH + ROOH = R'S-S-R' + H_2O + ROH$) was carried out in order to eliminate the metabolically produced peroxide by using thioredoxin as a hydrogen donor, which played an important role in anti-oxidation mechanism of injury.

Shigella was Gram-negative, facultative anaerobic and non-sporulating, which could infect humans and primates [10]. It was one of the main pathogens of bacterial dysentery. According to WHO (World Health Organization), the pathogen caused 164.7 million infected and 1.1 million deaths worldwide each year, most of which were children under 5 years old in developing countries. In China, more than 5 million cases were estimated per annum, which was caused by *Shigella flexneri* serotype 2a and most were associated with epidemic and pandemic shigellosis [11]. *Shigella* was highly invasive in the colon and the rectum. More than 95% of current clinical isolates appeared resistant to multiple antibiotics. The original vaccine was not ideal, which meant that effective prevention and treatment of diarrhea was a serious shortage. Therefore, developing the new anti-*Shigella* vaccine was one of the important work to the WHO [12]. The research may facilitate vaccine development and contribute to the treatment of dysentery causing by *Shigella*.

The crystal structures of some Prxs had been published, including four typical 2-Cys Prxs (Prx I, Prx II, TryP and AhpC), one atypical 2-Cys Prx (Prx V) and one 1-Cys Prx (Prx VI). These structures revealed Prxs to be very similar, each containing a thioredoxin fold with a few additional secondary-structure elements present as insertions. The most striking differences involved their oligomeric states. The atypical 2-Cys Prxs were monomeric enzymes, whereas both the typical 2-Cys and the 1-Cys Prxs were domain-swapped homodimers in which the C terminus of one subunit reaches across the dimer interface to interact with the other subunit [7]. SF2523 belonged to atypical 2-Cys, it represented a prototype of a novel type of mammalian peroxiredoxin. By amino acid sequence alignment, we could see that there were considerable differences between SF2523 and PrxV [13]. We focused on SF2523 protein gene cloning, expression, purification and preliminary crystallographic properties study, and aimed to provide

evidences for further revealing the physiological function and mechanism of peroxidase family.

1 Materials and methods

1.1 Macromolecule production

The expression vector pET-28b-SF2523 was produced as described by Feng *et al.* [14]. On the basis of the method described by Feng *et al.*, we adjusted the preparation and purification conditions of SF2523. Positive transformants were grown in 5 ml LB medium pH 7.0 containing 100 g/L kanamycin overnight at 310 K. 10 ml aliquots of the overnight culture were subcultured into 1 L fresh LB medium containing kanamycin (100 g/L). Protein expression was induced by addition of 0.2 mmol/L isopropyl-D-thiogalactopyranoside (IPTG) for 8–10 h at 289 K when the A_{600} reached 0.6–0.8. The cell pellet was harvested, resuspended and lysed by gentle sonication on ice for 10 min with phenylmethylsulfonyl fluoride (PMSF) added to the lysis buffer (20 mmol/L Tris-HCl pH 8.0, 500 mmol/L NaCl) to a final concentration of 1 mmol/L. The results show that recombinant SF2523 was only detected in the supernatant.

The clear supernatant of the protein solution after centrifugation was applied directly onto a 3 ml Ni Sepharose Fast Flow column (GE Healthcare) equilibrated with buffer (20 mmol/L Tris-HCl pH 8.0, 500 mmol/L NaCl). The contaminant proteins were washed out with washing buffer (20 mmol/L Tris-HCl pH 8.0, 500 mmol/L NaCl, 20 mmol/L imidazole). Finally, the target protein was eluted with elution buffer (20 mmol/L Tris-HCl pH 8.0, 100 mmol/L NaCl, 250 mmol/L imidazole). The major protein peak was collected, concentrated to 2 ml and applied onto a Superdex G200 (GE Healthcare) size-exclusion chromatography (SEC) column equilibrated with buffer consisting of 20 mmol/L Tris-HCl pH 8.0, 100 mmol/L NaCl. The target peak was collected and concentrated to 1 g/L for crystallization. All of the purification procedures described above was conducted at 277 K.

1.2 Crystallization, data collection and processing

Initial screening for crystallization conditions took place in 48-well sitting-drop plate at 289 K using the commercially available kits from Hampton Research (Crystal Screen, Crystal Screen 2, Index, PEG Rx1, PEG Rx2, PEG/Ion and PEG/Ion2). 1 μ l 1 g/L protein solution was mixed with an equal amount

of reservoir solution and equilibrated against 60 μ l reservoir solution. Sheet-shaped crystals appeared after 60 d in Index condition No.21 at 289 K (Figure 1). Detailed information on SF2523 crystallization was given in Table 1.

The harvested crystals were quickly mounted on the goniometer in a nitrogen stream at 100 K. Data were collected using a MAR 165 mm CCD detector on beamline 3W1A at the BSRF synchrotron radiation source, Institute of High Energy Physics, Chinese Academy of Sciences. The data were indexed, integrated and scaled with HKL-2000^[15].

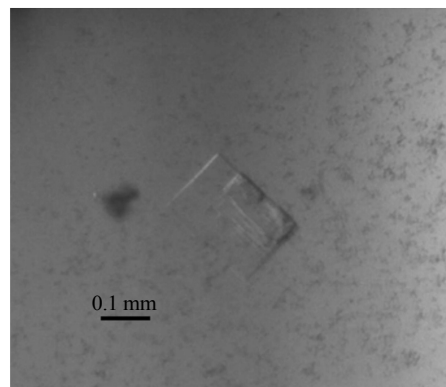


Fig. 1 Crystal of SF2523

Table 1 Crystallization conditions of SF2523

Method	Sitting-drop vapour diffusion
Plate type	48-well sitting drop
Temperature/K	289
$\rho(\text{protein})/(\text{g} \cdot \text{L}^{-1})$	1
Buffer composition of protein solution	20 mmol/L Tris-HCl pH 8.0, 100 mmol/L NaCl
Composition of reservoir solution	1.8 mol/L tri-Ammonium citrate, pH 7.0
Volume and ratio of drop	2 μ l, 1 : 1
Volume of reservoir	60 μ l

2 Results and discussion

The pET-28b-SF2523 co-expression system was constructed and SF2523 was expressed in *E. coli* BL21 (DE3) cells. SF2523 protein was found to have an apparent molecular mass of 19.7 ku. The results showed that recombinant SF2523 was only detected in the soluble cell fraction. SF2523 protein was purified to homogeneity, eluting as a symmetrical peak from the Superdex G200 column at 16.48 ml elution buffer. The target peak was collected and concentrated to 1 g/L for initial crystallization screening. In the present study, we showed that the SF2523 had enzyme activity *in vitro*.

We obtained successful crystallization using Index No.21 consisted of 1.8 mol/L tri-Ammonium citrate, pH 7.0. Subsequent optimizations were performed using 16-well hanging-drop plates, fine-tuning the pH in the range 6.0–8.0 and the tri-Ammonium citrate concentration in the range 1.4–2.2 mol/L produced crystals. A total of 360 images with an oscillation angle of 1 each were collected and

an exposure time of 60 s per frame (Figure 2). The data-collection statistics were listed in Table 2. The crystal belonged to space group $P2_12_12_1$, with unit-cell parameters $a = 35.80 \text{ \AA}$, $b = 50.63 \text{ \AA}$, $c = 88.52 \text{ \AA}$, $\alpha = \beta = \gamma = 90.00^\circ$. The asymmetric unit was estimated to contain one molecule of SF2523, with a corresponding Matthews coefficient of $2.03 \text{ \AA}^3/\text{u}$ and a solvent content of 39.56%.

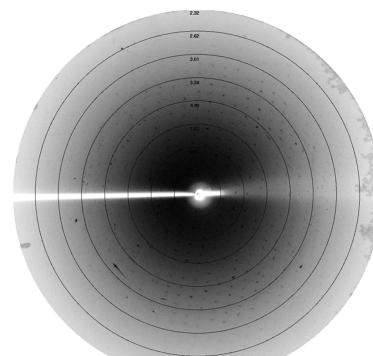


Fig. 2 An image of the SF2523 diffraction pattern to a resolution of 2.75 \AA

Table 2 Data collection and processing

Values for the outer shell are given in parentheses.

Diffraction source	3W1A, BSRF
Wavelength/Å	0.9792
Temperature/K	100
Detector	MAR CCD
Crystal-detector distance/mm	165
Rotation range per image/(°)	1
Total rotation range/(°)	360
Exposure time per image/s	60
Space group	P2 ₁ 2 ₁ 2 ₁
a, b, c/Å	35.80, 50.63, 88.52
α, β, γ /(°)	90.00, 90.00, 90.00
Mosaicity/(°)	3.07
Resolution range/Å	44.26–2.75(2.80–2.75)
Total No. of reflections	61 525
No. of unique reflections	4 496
Completeness/%	98.4(94.0)
Redundancy	13.7(7.6)
$\langle I/\sigma(I) \rangle$	13.85(2.17)
R_{rim}	26.4(50.4) ¹⁾
Overall B factor from Wilson plot /Å ²	19.3

¹⁾ R_{rim} was estimated by multiplying the conventional R_{merge} value by the factor $[N/(N-1)]^{1/2}$.

Sequence alignment of atypical 2-Cys Prxs showed that, although SF2523 and PrxV belonged to the same categories of Prxs, the amino acid sequences were quite different except of the conserved sequences of atypical 2-Cys Prxs (Figure 3). To get phasing information, we performed molecular replacement (MR) using the program MOLREP in the CCP4 program suite [16]. First, we used the published structures date of PrxV as models for MR, the trials with those models had failed. Then, we input the amino acid sequences of SF2523 into the SWISS-MODEL server. Among homologous structures searched by the SWISS-MODEL server, we selected 20 top-ranked crystal structures of exhibiting sequences identities of 35%–40% to SF2523 as potential search models. However, all MR trials with those models had failed. We used I-TASSER (Iterative Threading ASSEmbly Refinement) to search for structural templates no-showed in SWISS-MODEL server. One new template was used to perform MR, had failed. Data collection for selenium-derivatized SF2523 and crystal structure determination of SF2523 are in progress.

<i>Shigella</i>	-----MNPLKAGD
<i>Mus</i>	MLQLGLRVLGCKASSVL---RASTCLAGRAGRKEAGWECGGARSFSSSAVTMAPIKVG
<i>Homo</i>	MGLAGVLCALRRSAGYILVGGAGGQSAARRCSEGEWASGGVRSFSAAMAPIKVG
<i>Stygiella</i>	-----MLSSLKFNSIFSSVCGV---CVERAL---ASRF-LSLRAGGRVEKGD
<i>Xenopus</i>	-----MSVKVGD
	::**
<i>Shigella</i>	IAPKFSLE-QDGEQVNLTD-FQQRVLVYFYPKAMTPGCTV-QACGLRDNMDELKKAGV
<i>Mus</i>	AIPSEVFEGEPGKKVLAELFKGKVFCLSLGHLHLAVLR-PTAGFVEQAGALKAKGA
<i>Homo</i>	AIPAVEVFEGEPGNKVNLAELFKGKGVLFVPGPA
<i>Stygiella</i>	ELPDVVVFEGSPGNPKLRDVFAGKKGILFGVPGAFTPGCDKTHLPGYVKDFELFKKGV
<i>Xenopus</i>	QLPNVTVEGGPGNKVSIRDVFANKKGVLFVPGAFTPGCSKTHLPGYVAQAEELKSRGA
	* . : * * : * : : * : .
<i>Shigella</i>	DVLGIST-DKPEKLSRFAEKELLNFTLLSDEHDQVCEQFGVWGEKSFMGKTYDGIHRISF
<i>Mus</i>	QVVACLSVNDVFVI-----EEWGR-----AHQAEGKVRL
<i>Homo</i>	-----FTPSCSKVRL
<i>Stygiella</i>	EVIACVAVNDPFVM-----GAWGE-----AHAAQGVKVM
<i>Xenopus</i>	AVIACISVNDIFVM-----SEWAK-----AYDAEGKVC
	. : :
<i>Shigella</i>	LIDADGKIEH-----VFDDFKTSNHHDV-----VL
<i>Mus</i>	LADPTGAFGKATDLLLDDSLVSLFGNRRRLKRFMSVIDNGIVKALNVEPDGTGLTCSLAP
<i>Homo</i>	LADPTGAFGKETDLLLDDSLVSLFGNRRRLKRFMSVVDGIVKALNVEPDGTGLTCSLAP
<i>Stygiella</i>	LADTQATLAKALKLEFD---ATQVLGGIRCFERFSMIVNDNKVAFVNVPEPKVGLTCSLAN
<i>Xenopus</i>	LADPCGDFAKACGLLLDKKELSELFGNQCRKRFMSVVEDGKVKAINVEEDGTGLTCSLAG
	* * . : : : : : .
<i>Shigella</i>	NWLKEHA
<i>Mus</i>	NILSQL-
<i>Homo</i>	NIISQL-
<i>Stygiella</i>	VLLKEL-
<i>Xenopus</i>	NIMSQL-
	:::

Fig. 3 Sequence alignment of SF2523 from Shigella, and Prx V s from Mus, Homo, Stygiella and Xenopus

SF2523 sequence from Shigella (*Shigella boydii*, WP_001068689.1) and Prx V sequences from mouse (*Mus musculus*, AAF21016.1), human (*Homo sapiens*, AAI43850.1), Stygiella (*Stygiella incarcerate*, ANM86847.1) and Xenopus (*Xenopus tropicalis*, NP_001106525.1) were aligned by Clustal O.

Acknowledgement We thank Dr. Gao Zeng-qiang and coworkers of beamline 3W1A at the BSRF for their assistance during data collection.

References

- [1] Limauro D, Pedone E, Galdi I, *et al.* Peroxiredoxins as cellular guardians in *Sulfolobus solfataricus*: characterization of Bcp1, Bcp3 and Bcp4. The FEBS Journal, 2008, **275**(9): 2067–2077
- [2] Trachootham D, Lu W, Ogasawara M A, *et al.* Redox regulation of cell survival. Antioxidants & Redox Signaling, 2008, **10**(8): 1343–1374
- [3] Penta J S, Johnson F M, Wachsman J T, *et al.* Mitochondrial DNA in human malignancy. Mutation Research, 2001, **488**(2): 119–133
- [4] Poppek D, Grune T. Proteasomal defense of oxidative protein modifications. Antioxidants & Redox Signaling, 2006, **8** (1–2): 173–184
- [5] Ray P D, Huang B W, Tsuji Y. Reactive oxygen species (ROS) homeostasis and redox regulation in cellular signaling. Cellular Signalling, 2012, **24**(5): 981–990
- [6] Dietz K J, Jacob S, Oelze M L, *et al.* The function of peroxiredoxins in plant organelle redox metabolism. Journal of Experimental Botany, 2006, **57**(8): 1697–1709
- [7] Wood Z A, Schroder E, Robin Harris J, *et al.* Structure, mechanism and regulation of peroxiredoxins. Trends in Biochemical Sciences, 2003, **28**(1): 32–40
- [8] Limauro D, D'ambrosio K, Langella E, *et al.* Exploring the catalytic mechanism of the first dimeric Bcp: Functional, structural and docking analyses of Bcp4 from *Sulfolobus solfataricus*. Biochimie, 2010, **92**(10): 1435–1444
- [9] Clarke D J, Ortega X P, Mackay C L, *et al.* Subdivision of the bacterioferritin comigratory protein family of bacterial peroxiredoxins based on catalytic activity. Biochemistry, 2010, **49**(6): 1319–1330
- [10] Jin Q, Yuan Z, Xu J, *et al.* Genome sequence of *Shigella flexneri* 2a: insights into pathogenicity through comparison with genomes of *Escherichia coli* K12 and O157. Nucleic Acids Research, 2002, **30**(20): 4432–4441
- [11] Wang X Y, Tao F, Xiao D, *et al.* Trend and disease burden of bacillary dysentery in China (1991–2000). Bulletin of the World Health Organization, 2006, **84**(7): 561–568
- [12] Sansonetti P J. Slaying the Hydra all at once or head by head? Nature Medicine, 1998, **4**(5 Suppl): 499–500
- [13] Declercq J P, Evrard C, Clippe A, *et al.* Crystal structure of human peroxiredoxin 5, a novel type of mammalian peroxiredoxin at 1.5 Å resolution. Journal of Molecular Biology, 2001, **311**(4): 751–759
- [14] Feng D, Zhang K, Li Q, *et al.* Expression, purification, activity detection and crystal growth studies on Sf2523 protein from *Shigella flexneri* 2a strain 301. Journal of Chinese Biotechnology, 2012, **32**(8): 24–29
- [15] Otwinowski Z, Minor W. Processing of X-ray diffraction data collected in oscillation mode. Methods in Enzymology, 1997, **276**(20): 307–326
- [16] Collaborative Computational Project N. The CCP4 suite: programs for protein crystallography. Acta Crystallographica Section D, Biological Crystallography, 1994, **50**(Pt 5): 760–763

福氏志贺菌硫氧还过氧化物酶的 晶体生长和初步晶体学研究^{*}

刘 永¹⁾ 鲁 芳²⁾ 郭刚兴¹⁾ 冯 舵¹⁾ 张 蓓¹⁾ 高 伟^{1)**} 毕汝昌³⁾

(¹⁾北京林业大学理学院, 北京 100083; (²⁾北京林业大学林学院, 北京 100083; (³⁾中国科学院生物物理研究所, 北京 100101)

摘要 过氧化物酶是一类广泛存在于生物体内的抗氧化剂, 清除有氧代谢过程中产生的活性氧, 对于保护机体内的生物大分子有重要的生物学功能. 福氏志贺菌硫氧还过氧化物酶(SF2523)作为过氧化物酶家族的一员, 通过清除福氏志贺菌体内的活性氧, 在维持其活性和致病性上起重要作用. 目前, SF2523 的三维结构还没有得到解析, 其具体的功能机制也尚不清楚. 为了得到 SF2523 蛋白的三维结构, 进而了解具体的功能机制, 实验获得了均一稳定的可溶蛋白, 验证具有体外活性, 培养出可用于 X 射线衍射的蛋白质晶体. 在中国科学院高能物理研究所同步辐射装置收到晶体的衍射数据供结构解析使用. SF2523 晶体属于空间群 $P2_12_12_1$, 晶胞参数为 $a = 35.80 \text{ \AA}$, $b = 50.63 \text{ \AA}$, $c = 88.52 \text{ \AA}$, $\alpha = \beta = \gamma = 90.00^\circ$, 每个晶体学不对称单位含有 1 个蛋白质分子, 马修斯系数为 $2.03 \text{ \AA}^3/\text{u}$, 溶剂含量为 39.56%.

关键词 硫氧还蛋白过氧化物酶, 活性氧, 晶体

学科分类号 Q6, Q7

DOI: 10.16476/j.pibb.2017.0067

^{*} 中央高校基本科研业务费专项资金(2015ZCQ-LY-02)和国家自然科学基金(31070651)资助项目.

^{**} 通讯联系人.

Tel: 010-62338136, E-mail: w_gao@bjfu.edu.cn

收稿日期: 2016-09-08, 接受日期: 2017-03-06